First Principle Analysis of Charge Dissociation and Charge Recombination Processes in Organic Solar Cells

Velardo, Amalia; Borrelli, Raffaele; Capobianco, Amedeo; La Rocca, Mario Vincenzo; Peluso, Andrea. First Principle Analysis of Charge Dissociation and Charge Recombination Processes in Organic Solar Cells. JOURNAL OF PHYSICAL CHEMISTRY. C, NANOMATERIALS AND INTERFACES. 119 (33) pp: 18870-18876.
DOI: 10.1021/acs.jpcc.5b04038

The Absorption Band Shapes of a Push-Pull Dye Approaching the Cyanine Limit: A Challenging Case for First Principle Calculations of Ground and Excited State Molecular Properties in Solution

Amedeo Capobianco,*,† Raffaele Borrelli,‡ Alessandro Landi,† Amalia Velardo,† and Andrea Peluso*,†

†*Dipartimento di Chimica e Biologia, Università di Salerno, Via G. Paolo II, I-84084 Fisciano (SA), Italy*

‡*b) Dipartimento di Scienze Agrarie, Forestali e Alimentari, Università di Torino, Largo Paolo Braccini, 2. I-10095 Grugliasco (TO), Italy*

E-mail: acapobianco@unisa.it; apeluso@unisa.it

Abstract

The absorption band shapes of a donor-acceptor dye whose electronic structure can be finely tuned from push-pull to cyanine limit upon changing solvent polarity, have been theoretically investigated by using Kubo's generating function approach, with minimum energy geometries and normal modes computed at DFT level of theory. The comparison of the observed and predicted absorption band shapes and the analysis of dipole moment variations upon excitation reveal that a delicate balance of Hartree-Fock exchange in the functional is needed to treat such a difficult systems by density

functional theory, band shapes being nearly qiantitatively reproduced by using range separated hybrid functionals with high percentage of Hartree-Fock exchange.

Introduction

Organic donor-acceptor dyes with electronic structures approaching the cyanine limit have found applications in several technological fields, such as dye sensitized and bulk heterojunction solar cells,[? ?] optical storage media,[?] and nonlinear optics.[? ? ?] Highly reliable computational approaches are therefore needed for a deeper understanding of their electronic structures and for a rational design of new ones, but the easily polarizable electronic clouds of those compounds make them problematic and challenging systems for most of the computational approaches for large size molecules.[? ? ?] It has been shown that computational approaches based on time dependent density functional theory (DFT) predict vertical excitation energies which significantly disagree with the location of the absorption maxima of the experimental spectra in solution. The observed discrepancy can be partly ascribed to an insufficient description of double-excitations at TDDFT level,[? ?] and partly imputed to nuclear relaxations upon excitation, which make it inaccurate any comparison between vertical transition and experimental ansorption peaks.[?] Simulations of the whole absorption band shapes are therefore necessary for better assessing the reliability of electronic computations. Such simulations can also provide useful information about the accuracy with which computational approaches predict excited state geometries, which in turns control the rates of the photochemical processes which make those compounds of technological interest.[1] Herein we report first principle calculations of the band shape of the donor-acceptor XXYYZZ (**1**) dye, see scheme 1, which represents a very interesting test case because its absorption spectrum strongly depends on the polarity of the solvent, exhibiting not only a red-shift of the absorption maximum but also a remarkable change of the whole band shape.[2]

In non-polar solvent, such as diethyl ether, the absorption spectrum of compound **1** is

characterized by two well resolved peaks, falling in dioxane at 15385 and 16491 cm^{-1} and possessing roughly the same intensity, see Figure 1. As the solvent polarity increases, the longer wavelength absorption gains intensity and shifts to lower frequencies (ca 15110 cm^{-1} in acetonitrile, Figure 1, orange line), whereas the shorter wavelength absorption looses intensity and becomes a shoulder in strongly polar solvents such as acetonitrile (AN). The substantial change of the spectral shape and electrooptical absorption (EOA) measurements suggest that in weakly polar solvents **1** is a push-pull donor-acceptor system, with the neutral form prevailing in the ground state and the zwitterionic form in the excited one (see Scheme 1). Upon increasing the dielectric constant of the solvent, the contribution of the zwitterionic resonance form in the ground state increases, up to reaching the so called cyanine limit, with equally weighted neutral and zwitterionic resonance forms both in the ground and in the first excited state, in acetonitrile, where **1** exhibits a sharp and intense absorption band, typical of cyanine dyes.[2]

Computational procedure

A wide panel of methods has been employed for density functional and time dependent (TD) density functional theory (DFT) computations. Pure and global hybrid GGA and meta GGA exchange-correlation potentials have been considered. We have also used range separated hybrid functionals, i.e. hybrid functionals in which the exchange component is divided into short-range (SR) and long-range (LR) parts by splitting the Coulomb operator via the error function:[3]

$$\frac{1}{r_{12}} = \underbrace{\frac{1-[\alpha+\beta\,\mathrm{erf}\,(\omega r_{12})]}{r_{12}}}_{\mathrm{SR}} + \underbrace{\frac{\alpha+\beta\,\mathrm{erf}\,(\omega r_{12})}{r_{12}}}_{\mathrm{LR}} \tag{1}$$

The DFT exchange interaction is included through the first term, while the long-range orbital-orbital exchange interaction is described with the Hartree-Fock (HF) exchange inte-

gral. The parameter $0 \leq \alpha \leq 1$ is the fraction of HF exchange which contributes over the whole range; the parameter β incorporates the DFT counterpart over the whole range by a factor of $1 - \alpha - \beta$ and acts in such way that $\alpha + \beta$ is the fraction of HF exchange in the asymptotic limit; ω defines the range of the separation: the larger its value, the sharper is SR-LR separation.

Default settings have been used for range separated functionals except for CAM*, a modification of CAM-B3LYP in which a larger fraction of HF exchange has been imposed by increasing the α and β parameters up to 0.30 and 0.60 respectively, while leaving ω at its default (0.33 bohr^{-1}), see ref. 3 and Table 1.

Effects due to solvent polarization were included by the polarizable continuum model (PCM).[4] The non-equilibrium solvation scheme in which the effects of the slow motion of the solvent are not included has been used for excited states.[5] The 6-31+G(d,p) basis set was employed for DFT and TDDFT computations because it provides reliable ground and excited state equilibrium geometries and dipole moments.[6–8]

Frozen core (PCM)MP2/6-31+G(d) computations of ground state dipole moments were also carried out to have reference values for the solvents in which EOA measurements are not available. MP2 was chosen because it is known to give reliable dipole moments,[9] even for donor-acceptor systems.[7,8] The Gaussian package was used for MP2, DFT and TDDFT calculations.[10] The butyl chains of **1** (Scheme 1) have been replaced by methyl groups in all the calculations.

Band shapes have been evaluated by means of the generating function (GF) approach,[11? ? ? ? –13] which provides several advantages with respect to the standard recursive calculation of Franck-Condon factors,[14? ?] inasmuch as it allows to include in computations the whole set of the molecular normal modes, taking into account both the effects due to changes of the equilibrium position and of vibrational frequencies, as well as the effects due to normal mode mixing. Remarkably, the generating function approach does not pose any limitation on the number of modes which can be excited and on their highest quantum number, so that

the main limitation of the approach employed here in computing band shapes consists in neglecting anharmonic effects, which in principle can be included, but at high computational costs and for a few number of vibrational modes.[?]

Absorption spectra were computed by using a local development version of MolFC program.[14–16] The curvilinear coordinate representation of the normal modes has been adopted to prevent that displacements of angular coordinates could result into unrealistic shifts of stretching coordinates upon excitation.[17–19] That is unavoidable in the rectilinear Cartesian description and requires the use of high order anharmonic potentials for its correction.[20–22] Apart from the use of an apodization function in the Fast Fourier Transform, citeBorrelli12JPCA,Borrelli13CJC,Borrelli11PCCP no external adjustable parameters such as different Gaussian fitting functions for each different vibronic line have been used, thus ensuring a very effective test of the performances of the electronic calculations.

Results

Dipole moments and BLA

In its most stable *Z* configuration, chromophore **1** can assume the *s-trans* and *s-cis* conformations shown in Scheme 2. The predicted relative energies are reported in Table 2: *s-trans* conformation is more stable than *s-cis* one according to all the tested methods, in line with ^{1}H-NMR data.[23] The stability of the *s-trans* form should increase with the polarity of the solvent **Perché**.

Experimental and computed ground and excited state dipole moments of **1** are reported in Table 3. Dipole moment variation upon excitation to the first excited state ($\Delta\mu = \mu_{\mathrm{exc}} - \mu_{\mathrm{gr}}$) is predicted to decrease by increasing the field strength of the solvent by all functionals, in agreement with the experimental evidence. Both ground and excited state dipole moments increase upon increasing the polarity of the solvent, but μ_{gr} increases at a larger extent because, as indicated by its vanishing bond alternation lenght (BLA), the excited state is

strongly polarized already in the gas phase (**mancano i valori di BLA per l'eccitato)**.

The fraction of exact exchange in the functional plays a role opposite to the polarity of the environment on ground state dipole moments: Ground state dipole moments predicted to decrease upon increasing HF exchange; indeed by mitigating the self-interaction error a better agreement with experimental outcomes and MP2 predictions is achieved, in accord with previous results.[7,8,24] By contrast, an increase of the fraction of HF exchange in the functional results in a more polarized excited state; as an example, the excited state dipole moment is predicted to increase on average by ≈ 1 D in passing form B3LYP to ωB97X, see Table 3. This in turn causes an increase of $\Delta\mu$ with the increase of exact exchange. In summary, only functionals possessing a high fraction of HF exchange are capable of properly describing the electron density of **1** in weakly polar environment, where experimental evidence shows that **1** behaves like a push-pull donor-acceptor. Instead, pure and low-exchange functionals erroneously predict that **1** reaches a cyanine limit electronic configuration, independently of solvent polarity. That is clearly shown by the computed ground state BLA reported in Table 4. The BLA and hence the push-pull character of **1** is predicted to decrease with the polarity of the environment, in such way that the cyanine limit condition (BLA ≈ 0) is approximatively met in acetonitrile according to all functionals. For all the environments, the BLA increases upon increasing the fraction of exact exchange in the functional,[25,26] as seen e.g. by B3LYP and CAM* estimates in dioxane, amounting to 0.02 and 0.05 Å, respectively. In particular, only functionals giving BLA $\geq 5 \times 10^{-2}$ Å are capable of reproducing the observed $\Delta\mu$ in low-polarity environments.

Band shapes

Since UV/Vis absorption spectra are known to exhibit only a marginal dependence on conformations, we have first of all considered the most stable *s-trans* conformer, c.f. Table 2.

The UV/vis absorption spectrum of **1** recorded in diethyl ether (Figure 1, thick black line)

spans a range of ca. 7000 cm^{-1}, starting at ca. 14000 cm^{-1} and reaching its largest intensity between 15000 and 17000 cm^{-1}. The absorption band is characterized by two well resolved peaks, at ca. 15450 and 16500 cm^{-1}. The two peacks possess nearly the same intensity and are separated by a minimum falling at ca. 16000 cm^{-1} with $\sim 90\%$ of maximum absorbance.

UV/Vis spectra obtained by PBE, M06-L, B3LYP and PBE0 functionals using diethyl ether as the solvent are reported in Figure 2a, together with the experimental spectrum (dashed line). The agreement between the simulated and the experimental absorption band is quite poor. Pure functionals as well as functionals with low fraction of HF exchange overestimate the intensity of the absorption at 15450 cm^{-1}, while a quite flat shoulder is obtained in place of the peak at 16500 cm^{-1}. Moreover a too rapid decay is predicted both in the starting and in the ending regions of the spectrum. Coherently with estimated $\Delta\mu$ (see Table 3), those methods which describe the electronic structure of **1** as that of a cyanine-like system also in diethyl ether provide narrow ansorption bands, rather similar to those observed in high polarity solvents, where **1** actually reaches the cyanine limit.

Experimentally, the intensity ratio between the higher and the lower energy absorption maxima of the UV/Vis spectrum increases up to ≈ 1 when merocyanine **io ancora non ho capito cos'è una merocianina, siamo sicuri che 1 lo è?)1** assumes a push-pull structure. The latter is computationally achieved by increasing the fraction of HF exchange (Tables 3 and 4) in the functional. Therefore spectra with higher intensity ratios better simulating the experimental band-shape are expected by increasing the fraction of HF exchange in the functional. This is indeed the case. Comparison of panels A and B of Figure 2 shows that CAM-B3LYP performs better than B3LYP. The two maxima and the hinted shoulder at 18000 cm^{-1} are found (Figure 2b, red line) by CAM-B3LYP computations, but the intensity ratio between the lowest and highest energy absorptions is overestimated, being ca 2.7. The comparison of B3LYP and CAM-B3LYP spectrum led us to modify the latter functional and introduce the CAM* functional which differs from CAM-B3LYP only for the larger amount of HF exchange (see Table 1). In the CAM* spectrum (Figure 2b, blue line), the peak

height ratio reduces to 1.9 and a slower decay is observed in the region of high wavenumbers, therefore a further improvement with respect to CAM-B3LYP is obtained by the CAM* functional, in line with with expectations.

Very similar results are obtained by M06-2X and CAM-B3LYP, and CAM* and ωB97X, respectively (see the Supporting Information), thus showing that the amount of exact exchange is more important than correlation to achieve a good accuracy for vibronic spectra for compound **1**.

In spite of the large improvement with respect to B3LYP, still the predicted spectrum by CAM* functional for diethyl ether somewhat resembles the experimental spectra recorded in higher polarity solvents (compare Figure 2b with Figure 1). A glance at Tables 3 and 4 suggests that polarization effects introduced by PCM for diethyl ether may be slightly overestimated. Since the spectra recorded in diethyl ether and the less polar 1,4-dioxane solvent are almost identical,[2] we have also carried out computations for 1,4-dioxane. Figure 2c shows that theoretical spectra using dioxane provide a closer agreement with experiment than those using diethyl ether as the solvent at both CAM-B3LYP and CAM* levels (compare Figures 2B and 2C). In passing from diethyl ether to dioxane, the predicted peak height ratio reduces to 1.2 according to CAM* computations and the energy shift between the two maxima lowers from 1650 to ca 1600 cm^{-1}, but still the maxima of the computed spectra are too distant and the intensity of the lower energy peak is too high.

To further enhance the push-pull character of **1**, we considered also the gas phase to mimic a scarcely polar environment. Figure 2d reports the spectra computed by using the ωB97X functional in conjunction with diethyl ether, 1,4-dioxane and the gas phase. Decreasing the extent of dielectric effects substantially improves the quality of the prediction. The computed peak height ratio is ca 2.0 for diethyl ether (Figure 2d, blue line), 1.2 for dioxane (Figure 2d, green line) and 1.0 for the gas phase (red line), the latter estimate being in excellent agreement with the experimental spectrum.

The gas phase spectrum predicted by ωB97X or CAM* functionals (see infra) strongly

resembles the experimental one, yet the energy difference between the two maximum absorption peaks is slightly overestimated (1430 vs 1000 cm^{-1}), and the simulated spectrum is slightly broader than the observed one, hinting at anharmonic effects. In Figure 2e the experimental spectrum has been superimposed to the gas-phase spectra obtained by ωB97X GF computations carried out by scaling the harmonic frequencies of the ground and the excited state by 0.95 (green line) and 0.90 (blue line). Upon decreasing the scaling factor (sf), the predicted spectrum becomes narrower and closer to the experimental one. The energy shift between maximum absorption peaks amounts to 1427 cm^{-1} in the unscaled spectrum, but it progressively decreases, reaching 1260cm^{-1}at sf = 0.90, while the peak height ratio remains substantially unchanged. Although the use of the same scaling factor for all the vibrational modes is a poor approximation,,[27] results collected in Figure 2e constitute a reasonable indication that the small discrepancies between the computed and the experimental spectrum can be ascribed at least in part to anharmonic effects.

In weakly polar environment *s-cis* should be less stable than *s-trans* conformer by only $\approx$ 1 kcal/mol according to CAM* and ωB97X functionals (Table 2). Given that exiguous energy difference close to calculation accuracy, it is likely that *s-cis* is sufficiently populated to be detected at room temperature. We have therefore also computed the spectrum of the cis conformer for low polarity environments (gas and dioxane) by using the best performing functionals (CAM* and ωB97X). Figure 2e reports the gas-phase spectra obtained at the CAM* level for *s-trans* and *s-cis* conformers. Although both conformers share a large portion of the spectrum, the higher energy peak is comparably more intense for **1**/*s-cis*. This suggests that the agreement between the predicted and experimental spectrum could be further improved by considering both conformations. The same also holds for 1,4-dioxane, see Figure SYY in the Supporting Information.

Computed and experimental absorption spectra in acetonitrile are reported in Figure 3. In agreement with experimental evidence, band widths are predicted to be narrower and less structured than those estimated for weakly polar solvents (compare with Figure 2) by all

functionals, thus indicating that **1** is actually reaching the cyanine limit. This in line with dipole moments and BLA parameters of Tables 3 and 4. With the exception of PBE, all the functionals obtain a reasonably accurate spectrum, but still high-exchange functionals, such as M06-2X, CAM-B3LYP or ωB97X ensure the best agreement with the experiment.[28]

Absorption energies

Table 5 shows that vertical transition energies are systematically overestimated with respect to experimental maximum absorption energies; the poor performance on the prediction of reliable excitation energies for cyanine is a well documented issue, which is known to affect the quality of almost all the computational methods, not only TDDFT.[29] Present results show that high exchange functionals such as ωB97X overestimate transition energies by ca 0.55 eV; a lower error, ca 0.4 eV, is obtained by pure and low-exchange GGA functionals. Note however that for all environments and functionals, vertical energies are larger, up to 0.3 eV, than absorption energies taken at the maximum intensity of the computed spectrum, so that a better agreement with experiment is obtained if one correctly compares computed and experimental maximum absorption energies. For compound **1**, the computation of the vibronic shape is therefore a necessary effort to make a meaningful comparison of experimental and predicted transition energies, as also noted for other systems.[13,28,30]

Notably, maximum absorption energies are predicted to coincide within 0.01 eV with E_{00}, showing that $0 \leftarrow 0$ is a very intense transition. This is in line with the expectation that comparatively small structural changes are involved in the CT transition of a cyanine dye, as also confirmed by the RMSD's between ground and excited state equilibrium geometries, being $\lessapprox 0.1$ Å for all the investigated cases.

Polarization effects introduced by PCM for low polarity solvents may appear slightly overestimated as noted for the band shapes in diethyl ether (see above) or by arguing that predicted maximum absorption energies of Table 5 remain substantially unaltered in passing form 1,4-dioxane to the more polar acetonitrile solvent according to all the tested functionals.

However this is not a drawback if one notices that the solvatochromic effect (Figure 1 and Table 5) covers a very small energy range, ca 0.05 eV, close to computational accuracy.

Forse qui si potrebbero fare delle chiacchiere sul fatto che non abbiiamo utilizzato i modelli di solvatazione PCM raffinati per trattare gli stati eccitati, ma il loro beneficio è messo in dubbio dagli stessi autori, e poi, al momento i gradienti analitici non sono stati implementati, quindi è impossibile pensare di calcolare i FC con tali metodi.

Conclusions

The solvatochromic behavior of a donor-acceptor dye shifting from push-pull to a cyanine-like condition upon increasing the polarity of the environment has been investigated by computing the Franck-Condon spectra at the PCM/(TD)DFT level with the generating function approach. Computations of band-shapes appear to be a necessary effort for choosing the best electronic method for such a difficult case. Relying on the best agreement between vertical and experimental maximum absorption energy may be a misleading criterion, above all for low polarity environment where the push-pull form is dominating. In fact the push-pull regime is the most difficult case to treat with computations. Pure and low-exchange functionals erroneously assign a cyanine-like character to chromophore **1** in diethyl ether. Instead, high-exchange functionals are able to correctly reproduce the shape of the UV/Vis spectrum and to predict dipole moment variations in line with observations, which assign a push-pull character to compound **1**. A better agreement is obtained for the cyanine regime, reached in strongly polar solvents such as acetonitrile.

Excitation energies are systematically overestimated by all the tested functionals for all the environments.

Acknowledgments

INSERT

References

(1) Velardo, A.; Borrelli, R.; Capobianco, A.; La Rocca, M. V.; Peluso, A. First Principle Analysis of Charge Dissociation and Charge Recombination Processes in Organic Solar Cells. *J. Phys. Chem. C* **2015**, *119*, 18870–18876.

(2) Würthner, F.; Archetti, G.; Schmidt, R.; Kuball, H.-G. Solvent Effect on Color, Band Shape, and Charge-Density Distribution for Merocyanine Dyes Close to the Cyanine Limit. *Angew. Chem. Int. Ed.* **2008**, *47*, 4529–4532.

(3) Yanai, T.; Tew, D. P.; Handy, N. C. A New Hybrid Exchange-Correlation Functional Using the Coulomb-Attenuating Method (CAM-B3LYP). *Chem. Phys. Lett.* **2004**, *393*, 51–57.

(4) Miertuš, S.; Scrocco, E.; Tomasi, J. Electrostatic Interaction of a Solute with a Continuum. A Direct Utilization of Ab Initio Molecular Potentials for the Prevision of Solvent Effects. *Chem. Phys.* **1981**, *55*, 117–129.

(5) Barone, V.; Ferretti, A.; Pino, I. *Phys. Chem. Chem. Phys.* **2012**, *14*, 16130–16137.

(6) Charaf-Eddin, A.; Planchat, A.; Mennucci, B.; Adamo, C.; Jacquemin, D. Choosing a Functional for Computing Absorption and Fluorescence Band Shapes with TD-DFT. *J. Chem. Theory Comput.* **2013**, *9*, 2749–2760.

(7) Capobianco, A.; Centore, R.; Noce, C.; Peluso, A. Molecular Hyperpolarizabilities of Push-Pull Chromophores: A Comparison between Theoretical and Experimental Results. *Chem. Phys.* **2013**, *411*, 11–16.

(8) Capobianco, A.; Centore, R.; Fusco, S.; Peluso, A. Electro–Optical Properties from CC2 Calculations: A Comparison between Theoretical and Experimental Results. *Chem. Phys. Lett.* **2013**, *580*, 126–129.

(9) Hellweg, A. The Accuracy of Dipole Moments from Spin-Component Scaled CC2 in Ground and Electronically excited dipole Moments. *J. Chem. Phys.* **2011**, *133*, 064103–9.

(10) Frisch, M. J.; Trucks, G. W.; Schlegel, H. B.; *al*, E.-T. Gaussian 09 Revision D.01. Gaussian Inc. Wallingford CT 2009.

(11) Kubo, R.; Toyozawa, Y. Application of the Method of Generating Function to Radiative and Non-Radiative Transitions of a Trapped Electron in a Crystal. *Prog. Theor. Phys.* **1955**, *13*, 160–182.

(12) Lax, M. The Franck-Condon Principle and Its Application to Crystals. *J. Chem. Phys.* **1952**, *20*, 1752–1760.

(13) Avila Ferrer, F. J.; Cerezo, J.; Stendardo, E.; Improta, R.; Santoro, F. Insights for an Accurate Comparison of Computational Data to Experimental Absorption and Emission Spectra: Beyond the Vertical Transition Approximation. *J. Chem. Theory Comput.* **2013**, *9*, 2072–2082.

(14) Borrelli, R.; Peluso, A. Dynamics of Radiationless Transitions in Large Molecular Systems: A Franck-Condon Based Method Accounting for Displacements and Rotations of all the Normal Coordinates. *J. Chem. Phys.* **2003**, *119*, 8437–8448.

(15) Borrelli, R.; Peluso, A. MolFC: A program for Franck-Condon integrals calculation. Package available online at `http://www.theochem.unisa.it`.

(16) Borrelli, R.; Capobianco, A.; Peluso, A. Franck-Condon Factors: Computational Approaches and Recent Developments. *Can. J. Chem.* **2013**, *91*, 495–504.

(17) Borrelli, R.; Peluso, A. The Vibrational Progressions of the N $\rightarrow$ V Electronic Transition of Ethylene. A Test Case for the Computation of Franck-Condon Factors of Highly Flexible Photoexcited Molecules. *J. Chem. Phys.* **2006**, *125*, 194308–8.

(18) Borrelli, R.; Peluso, A. Erratum: "The Vibrational Progressions of the N$\leftarrow$V Electronic Transition of Ethylene: A Test Case for the Computation of Franck-Condon Factors of Highly Flexible Photoexcited Molecules". *J. Chem. Phys.* **2013**, *139*, 159902–1.

(19) Capobianco, A.; Borrelli, R.; Noce, C.; Peluso, A. Franck-Condon Factors in Curvilinear Coordinates: the Photoelectron Spectrum of Ammonia. *Theor. Chem. Acc.* **2012**, *131*, 1181.

(20) Peluso, A.; Borrelli, R.; Capobianco, A. Photoelectron Spectrum of Ammonia, a Test Case for the Calculation of Franck–Condon Factors in Molecules Undergoing Large Geometrical Displacements upon Photoionization. *J. Phys. Chem. A* **2009**, *113*, 14831–14837.

(21) Peluso, A.; Borrelli, R.; Capobianco, A. Correction to "Photoelectron Spectrum of Ammonia, a Test Case for the Calculation of Franck-Condon Factors in Molecules Undergoing Large Geometrical Displacements upon Photoionization". *J. Phys. Chem. A* **2013**, *117*, 10985–10985.

(22) Hoy, A. R.; Mills, I. M.; Strey, G. Anharmonic Force Constant Calculations. *Molec. Phys.* **1972**, *24*, 1265–1290.

(23) Würthner, F.; Thalacker, C.; Matschiner, R.; Lukaszuk, K.; Wortmann, R. Optimization of Neutrocyanine Chromophores Based on Five-membered Heterocycles for Photorefractive Applications. *Chem. Commun.* **1998**, 1739–1740.

(24) Centore, R.; Fusco, S.; Peluso, A.; Capobianco, A.; Stolte, M.; Archetti, G.; Kuball, H.-G. Push-Pull Azo-Chromophores Containing Two Fused Pentatomic Heterocycles and Their Nonlinear Optical Properties. *Eur. J. Org. Chem.* **2009**, 3535–3543.

(25) Jacquemin, D.; Adamo, C. Bond Length Alternation of Conjugated Oligomers: Wave Function and DFT Benchmarks. *J. Chem. Theory Comput.* **2011**, *7*, 369–376.

(26) Capobianco, A.; Velardo, A.; Peluso, A. DFT Predictions of the Oxidation Potential of Organic Dyes for Opto-Electronic Devices. *Comp. Theor. Chem.* **2015**, *1070*, 68–75.

(27) Capobianco, A.; Caruso, T.; Celentano, M.; La Rocca, M. V.; Peluso, A. Proton Transfer in Oxidized Adenosine Self-Aggregates. *J. Chem. Phys.* **2013**, *139*, 145101–4.

(28) Dierksen, M.; Grimme, S. Density Functional Calculations of the Vibronic Structure of Electronic Absorption Spectra. *J. Chem. Phys.* **2004**, *120*, 3544.

(29) Jacquemin, D.; Zhao, Y.; Valero, R.; Adamo, C.; Ciofini, I.; Truhlar, D. G. Verdict: Time-Dependent Density Functional Theory "Not Guilty" of Large Errors for Cyanines. *J. Chem. Theory Comput.* **2012**, *8*, 1255–1259.

(30) Send, R.; Valsson, O.; Filippi, C. Electronic Excitations of Simple Cyanine Dyes: Reconciling Density Functional and Wave Function Methods. *J. Chem. Theory Comput.* **2011**, *7*, 444–455.

(31) Perdew, J. P.; Burke, K.; Ernzerhof, M. Generalized Gradient Approximation Made Simple. *Phys. Rev. Lett.* **1996**, *77*, 3865–3868.

(32) Zhao, Y.; Truhlar, D. G. The M06 Suite of Density Functionals for Main Group Thermochemistry, Thermochemical Kinetics, Noncovalent Interactions, Excited States, and Transition Elements: Two New Functionals and Systematic Testing of Four M06-class Functionals and 12 Other Functionals. *Theor. Chem. Acc.* **2007**, *120*, 215–241.

(33) Becke, A. D. Density-Functional Thermochemistry. III. The Role of Exact Exchange. *J. Chem. Phys.* **1993**, *98*, 5648–5652.

(34) Stephens, P. J.; Devlin, F. J.; Chabalowski, C. F.; Frisch, M. J. Ab Initio Calculation of Vibrational Absorption and Circular Dichroism Spectra Using Density Functional Force Fields. *J. Phys. Chem.* **1994**, *98*, 11623–11627.

(35) Perdew, J. P.; Ernzerhof, M.; Burke, K. Rationale for Mixing Exact Exchange with Density Functional Approximations. *J. Chem. Phys.* **1996**, *105*, 9982–9985.

(36) Chai, J.-D.; Head-Gordon, M. Systematic Optimization of Long-Range Corrected Hybrid Density Functionals. *J. Chem. Phys.* **2008**, *128*, 084106–15.

(37) Liptay, W. Electrochromism and Solvatochromism. *Angew. Chem. Int. Ed.* **1969**, *8*, 177–188.

Table 1: Functionals used in the present work.

Functional	Type[a]	% HF exchange[b]	ref
PBE	GGA	0	31
M06-L	mGGA	0	32
B3LYP	GH-GGA	20	33,34
PBE0	GH-GGA	25	35
CAM-B3LYP	RSH-GGA	$19 \xrightarrow{0.33} 65$	3
M06-2X	GH-mGGA	54	32
CAM* [c]	RSH-GGA	$30 \xrightarrow{0.33} 90$	3
ωB97X	RSH-GGA	$16 \xrightarrow{0.30} 100$	36

[a]GGA = generalized gradient approximation, GH = global hybrid, RSH = range-separated hybrid, mGGA = meta-GGA. [b] The percentages of HF exchange in the short (left, α in eq. 1) and long range (right, $\alpha+\beta$ in eq. 1) limits are reported for RSH functionals; the parameter ω (bohr^{-1}) is reported over the arrow. [c] CAM-B3LYP with α and β set to 0.30 and 0.60, respectively.

Table 2: Predicted energy differences (kcal/mol) between *s-cis* and *s-trans* conformers of compound **2**. DX = 1,4-dioxane, DE = diethyl ether, AN = acetonitrile.

	gas	DX	DE	AN
PBE	1.3	1.4	1.4	1.5
B3LYP	1.0	1.2	1.3	1.4
CAM-B3LYP	0.9	1.1	1.2	1.4
M06-2X	1.4	1.6	1.8	2.0
CAM*	0.8	1.0	1.2	1.5
ωB97X	0.9	1.1	1.3	1.6
MP2	1.4	1.5	1.6	1.8

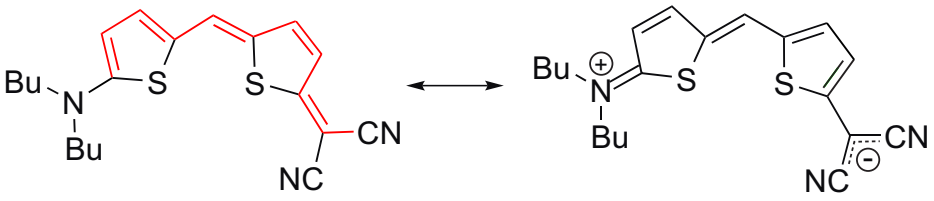

Scheme 1: The neutral (left) and zwitterionic (right) resonance forms of compound **1**. The path used to compute BLA has been highlighted in red.

Table 3: Computed and experimental ground (μ_g) and excited state (μ_e)[a] dipole moments (D). DX = 1,4-dioxane, DE = diethyl ether, AN = acetonitrile. Computations refer to *s-trans* conformation.

	gas		DX		DE		AN	
	μ_g	μ_e	μ_g	μ_e	μ_g	μ_e	μ_g	μ_e
PBE	14.6	15.0	18.5	18.6	21.0	20.8	24.4	23.6
M06-L	14.4	14.9	18.2	18.3	20.6	20.4	23.8	23.0
B3LYP	14.4	15.5	18.2	19.1	20.8	21.2	24.4	23.9
PBE0	14.2	15.5	18.0	19.0	20.6	21.1	24.2	23.6
CAM-B3LYP	13.3	16.3	16.9	19.9	19.5	21.9	23.9	24.1
M06-2X	12.7	16.0	16.2	19.6	18.7	21.6	22.7	23.7
CAM*	12.6	16.6	15.7	20.3	18.1	22.4	22.8	24.5
ωB97X	12.4	16.4	15.5	20.3	18.1	22.5	22.9	24.5
MP2	11.1	–	13.6	–	15.5	–	19.1	–
exper[b]	*11.2*	*16.7*	*14.0*	*19.0*	–	–	–	–

[a]Vertical approximation, see ref 37. [b]Ref. 2; gas phase values were obtained by using the Onsager model, see ref. 23.

Table 4: Predicted ground state BLA (10^{-2} Å).

	GAS	DX	DE	AN
PBE	2	2	1	0
M06-L	3	2	1	0
B3LYP	4	2	2	0
PBE0	4	2	2	0
CAM-B3LYP	5	4	3	0
M06-2X	5	4	3	0
CAM*	6	5	4	2
ωB97X	6	5	4	2

Table 5: Predicted maximum absorption (E_m), vertical (E_v) and E_{00} transition energies. All data are expressed in eV.

	gas			DX			AN		
	E_m	E_{00}	E_v	E_m	E_{00}	E_v	E_m	E_{00}	E_v
PBE	2.20	2.21	2.36	2.03	2.03	2.17	2.10	2.05	2.20
M06-L	2.34	2.25	2.50	2.17	2.17	2.31	2.17	2.19	2.33
B3LYP	2.36	2.38	2.53	2.17	2.17	2.31	2.19	2.19	2.32
PBE0	2.42	2.43	2.58	2.22	2.22	2.36	2.24	2.24	2.37
CAM-B3LYP	2.52	2.53	2.73	2.27	2.28	2.45	2.29	2.29	2.38
M06-2X	2.50	2.51	2.70	2.25	2.26	2.42	2.25	2.25	2.34
CAM*	2.66	2.66	2.95	2.39	2.39	2.63	2.38	2.39	2.46
ωB97X	2.60	2.60	2.88	2.33	2.32	2.56	2.31	2.32	2.38
exper.	–	–	–	*1.92*	–	–	*1.87*	–	–

Figure 1: UV/Vis absorption spectra of dye **1** in solvents of different polarity at 298 K ($c = 10^{-5}$ M). The thick black line is for the least polar solvent diethyl ether (in 1,4-dioxane the spectra are almost identical), blue line: ethyl acetate, purple line: tetrahydrofuran, red line: acetone, and orange line: acetonitrile. The arrow indicates the spectral shift with increasing solvent polarity. Reproduced with permission from ref 2. Copyright (2008) John Wiley and Sons.

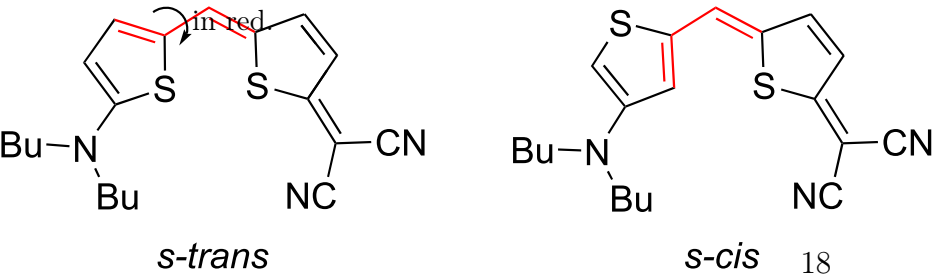

Scheme 2: *s-trans* and *s-cis* conformations of **1**. They differ for the torsion coordinate ω highlighted in red.

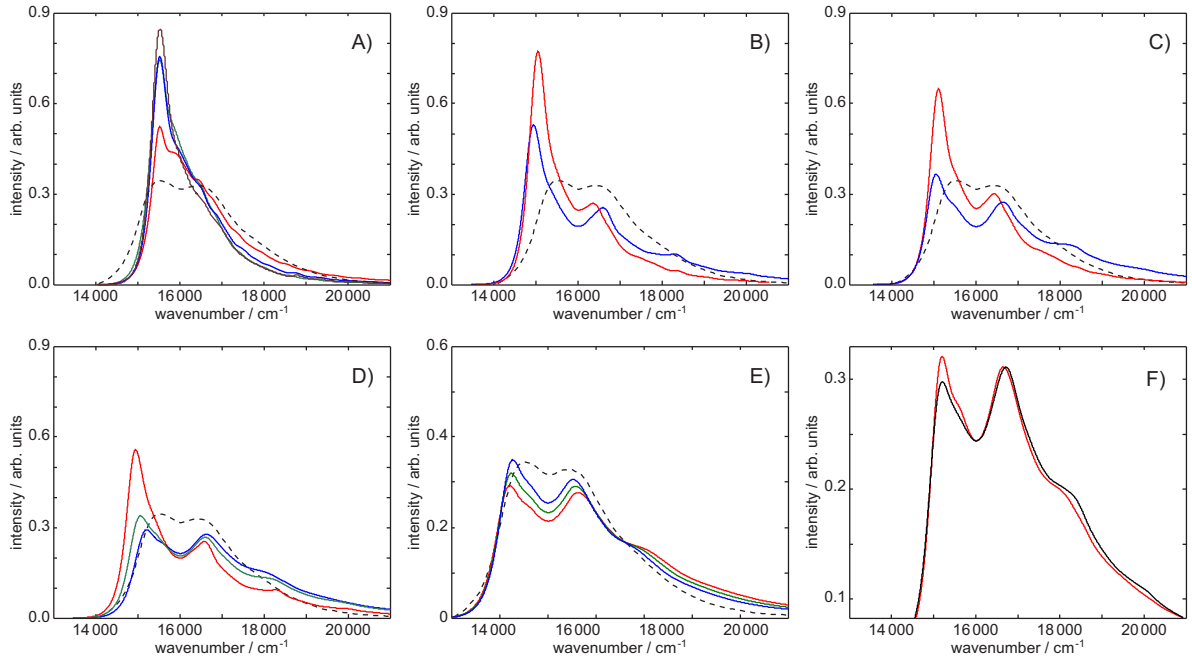

Figure 2: Predicted UV/absorption spectra of **1** in low polarity solvents. They refer to *s-trans* conformer, except where otherwise noted. Intensities have been scaled in such way that all the spectra possess the same area. The experimental spectrum recorded in DE has been superimposed as a dashed line. A): PBE(DE), red line; M06-L(DE), blue line; B3LYP(DE), green line. B): CAM-B3LYP(DE), red line; CAM*(DE), blue Line. C): CAM-B3LYP(DX), red line; CAM*(DX), blue Line. D) ωB97X(DE), blue line; ωB97X(DX), green line; ωB97X(gas), red line. E) ωB97X(gas) with differing scaling factors (sf): sf = 1, red line; sf = 0.95, green line; sf = 0.90, blue line. F) CAM*(gas), *s-trans* conformer, red line; *s-cis* conformer, black line.

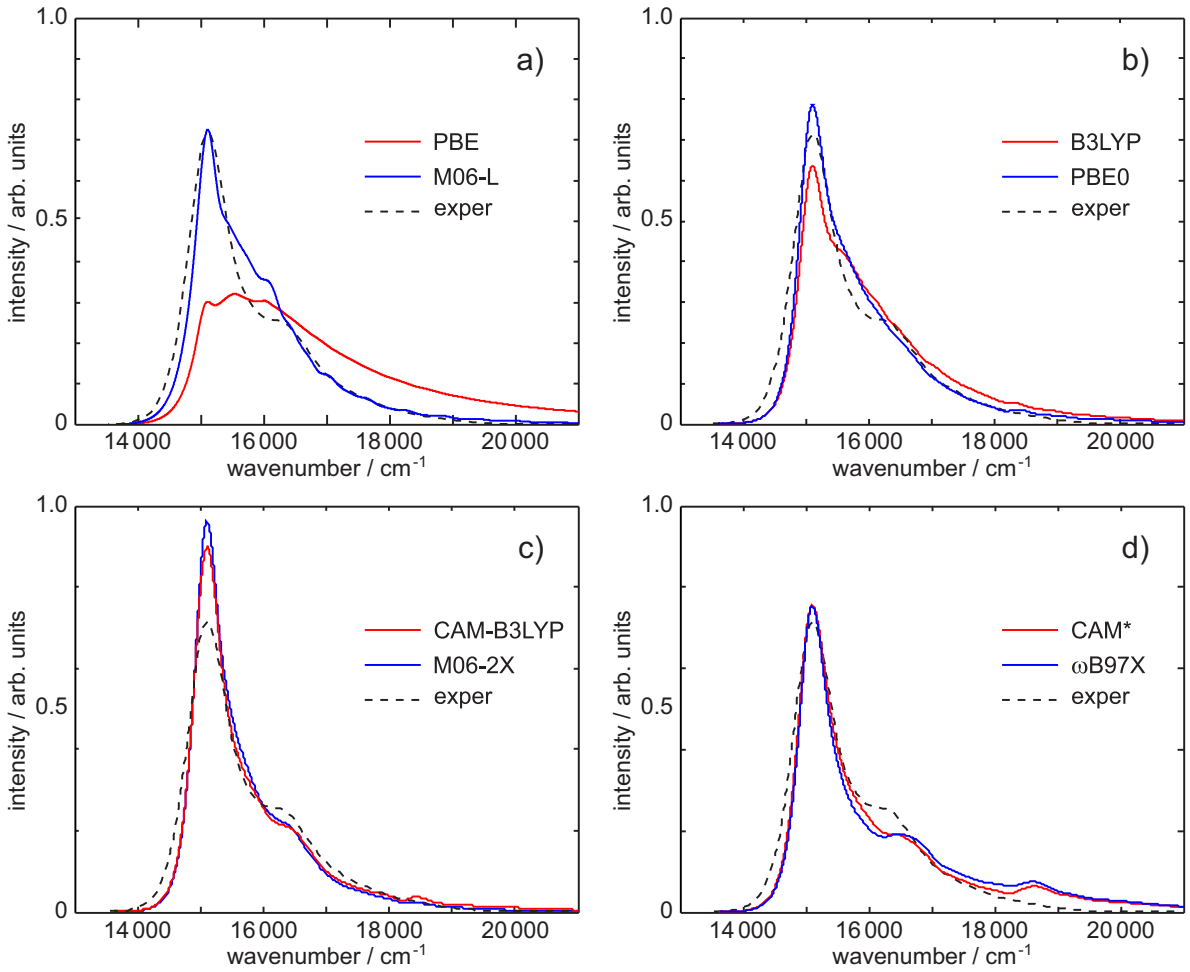

Figure 3: Predicted UV/absorption spectra of **1** in acetonitrile. The experimental spectrum has been superimposed as a dashed line. Panel a): PBE, red line; M06-L, blue line. Panel b): B3LYP, red line; PBE0, blue line. Panel c): CAM-B3LYP, blue line; M06-2X, red Line. Panel d) CAM*, red line; ωB97X, blue line.